

ORIGINAL ARTICLE

Mechanism of human PTEN localization revealed by heterologous expression in *Dictyostelium*

HN Nguyen, Y Afkari, H Senoo, H Sesaki, PN Devreotes and M Iijima

Phosphatase and tensin homolog (PTEN) is one of the most frequently mutated tumor suppressor genes in cancers. PTEN has a central role in phosphatidylinositol (3,4,5)-trisphosphate (PIP3) signaling and converts PIP3 to phosphatidylinositol (4,5)-bisphosphate at the plasma membrane. Despite its importance, the mechanism that mediates membrane localization of PTEN is poorly understood. Here, we generated a library that contains green fluorescent protein fused to randomly mutated human PTEN and expressed the library in *Dictyostelium* cells. Using live cell imaging, we identified mutations that enhance the association of PTEN with the plasma membrane. These mutations were located in four separate regions, including the phosphatase catalytic site, the calcium-binding region 3 (CBR3) loop, the C α 2 loop and the C-terminal tail phosphorylation site. The phosphatase catalytic site, the CBR3 loop and the C α 2 loop formed the membrane-binding regulatory interface and interacted with the inhibitory phosphorylated C-terminal tail. Furthermore, we showed that membrane recruitment of PTEN is required for PTEN function in cells. Thus, heterologous expression system in *Dictyostelium* cells provides mechanistic and functional insight into membrane localization of PTEN.

Oncogene advance online publication, 2 December 2013; doi:10.1038/onc.2013.507

Keywords: PTEN; membrane localization; mutational analysis; *Dictyostelium*

INTRODUCTION

Excessive phosphatidylinositol (3,4,5)-trisphosphate (PIP3) signaling caused by alternations in PI3K, phosphatase and tensin homolog (PTEN) or the PIP3-regulated serine/threonine kinase AKT leads to tumor formation and metastasis.^{1–3} Although PI3K inhibitors have been developed as anticancer drugs to suppress PIP3 production,^{4,5} activators of PTEN have not been explored. Despite the central role of PTEN in PIP3 signaling at the plasma membrane, the majority of PTEN is present in the cytosol and nucleus.^{6,7} Stimulating membrane localization of PTEN could potentially enhance its tumor suppressor function. Currently, the details of the mechanism of membrane localization are unclear.

PTEN has four distinct domains: an N-terminal lipid-binding domain, phosphatase domain, C2 domain and C-terminal tail domain (Figure 1a).^{7,8} The lipid binding, phosphatase and C2 domains can interact with phospholipids *in vitro*.^{9–11} Although the three dimensional structure of the phosphatase and C2 domains of PTEN has been revealed, the structure of the tail domain is not solved and proposed to be a flexible fragment.¹² The C-terminal tail binds the other part of PTEN and blocks its membrane association. This inhibitory, intramolecular interaction requires phosphorylation at S380, T382, T383 and S385 in the tail. When these residues were substituted with alanine (PTEN_{AA}), increased association with the plasma membrane and nucleus was observed in cells.^{9,13} In this study, we developed a heterologous expression system, in which human PTEN-GFP was expressed in *Dictyostelium* cells. Human PTEN is functional in *Dictyostelium* cells, as it rescues PTEN-null phenotypes.^{14–17} Using the powerful genetic system and accessible imaging of membrane localization afforded by expression in *Dictyostelium*, we defined the mechanism and regulation of human PTEN localization.

RESULTS

Human PTEN-green fluorescent protein (GFP) is mainly located in the cytosol of mammalian and *Dictyostelium* cells.^{9,15} We used error-prone PCR to generate a library of randomly mutated human PTEN complementary DNAs fused to GFP (complexity = 120 000, average mutation rate = 5.5 per molecule) and transfected the library into PTEN-null *Dictyostelium* cells. After selecting transformants in the presence of the antibiotic geneticin, we visually inspected ~20 000 colonies and collected 18 colonies that showed increased membrane association of PTEN-GFP (Figure 1a). After isolation of plasmids and DNA sequencing, the mutations were separated and re-examined for their effects on PTEN localization in *Dictyostelium* cells. Demonstrating the feasibility of our screen, we isolated mutations that have been reported to enhance membrane localization of PTEN (Figures 1a–c).^{9,15} These mutations were located in the catalytic site (cysteine at amino-acid residue 124 changed to arginine or serine, C124R/S) and in the C-terminal region that spans phosphorylation sites (amino-acid residues 380–385). The C-terminal mutations also increased nuclear localization. Combinations of C124R/S with the C-terminal mutations further increased membrane localization (Figures 1a–c), as previously described.¹³

It has been shown that phosphorylation of the C-terminal tail is important for the stability of PTEN.¹⁸ To examine the role of PTEN stability in its localization, we treated cells expressing either PTEN_{AA}, in which phosphorylation sites S380, T382, T383 and S385 were mutated to alanine, with a proteasome inhibitor, MG132 (Figures 1b–e). Intriguingly, membrane localization of PTEN_{AA}, but not its nuclear localization, was significantly enhanced. The localization of wild-type (WT) PTEN, which is mainly located in the cytosol, was not affected by MG132. Consistent with these

microscopic observations, quantification of immunoblotting showed that MG132 treatments increased the total amount of PTEN_{A4} but not WT PTEN (Figure 1f). We then asked whether increased membrane association of PTEN_{C124S/A4} resulted from increased stability of PTEN_{A4} by C124S. In contrast to PTEN_{A4}, membrane association of PTEN_{C124S} and PTEN_{C124S/A4} was not affected by MG132 (Figures 1b and c).

To further examine the effect of C124S and C-terminal phosphorylation sites mutations on PTEN localization, we inhibited protein synthesis using cycloheximide. Membrane association of PTEN_{A4} was selectively decreased by cycloheximide treatment and this decrease was rescued by C124S mutation (Figures 1b and c). Similarly, PTEN_{A4} showed a decreased half-life in the presence of cycloheximide and additional C124S mutation restored the normal protein stability (Figure 1g). These results suggest that PTEN at the plasma membrane is more sensitive to proteasome-mediated degradation and the mutation C124S confers increased resistance.

As C124 is required for the phosphatase activity of PTEN, we tested whether loss of catalytic activity stabilizes membrane association of PTEN_{A4}. Supporting this notion, another catalytic site mutation, R130G, also stabilized PTEN_{A4} at the membrane in the absence of MG132 (Figures 2a and b). However, in contrast to C124S, R130G alone did not increase membrane localization of PTEN. These data suggested that loss of phosphatase activity stabilizes membrane localization of PTEN_{A4} but alone is not sufficient to target PTEN to the membrane.

Previous studies have suggested that PTEN_{C124S} is a 'substrate-trapping' mutant that forms a stable complex with PIP3 at the plasma membrane.¹⁹ This model predicts that the membrane localization of PTEN_{C124S} depends on PIP3. To test the prediction, we treated cell with an inhibitor of PI3K, LY294002, which decreased PIP3 levels as shown by the loss of a PIP3 biosensor, PHcrac-GFP, from the plasma membrane (Figures 2c and d). However, membrane association of PTEN_{C124S} was not affected in LY294002-treated cells (Figures 2c and d). Similarly, membrane localization of PTEN_{C124S} was not affected in PTEN-null cells, in which PIP3 levels are increased (Figures 2c and d). These results suggest that membrane association of PTEN_{C124S} is independent of PIP3.

To explore whether, C124S has an additional role in membrane targeting, we examined interactions of PTEN with the C-terminal tail in pull-down assays (Figures 2e–g).⁹ In this assay, we expressed full-length PTEN as a GFP fusion in *Dictyostelium* cells. The C-terminal tail domain was tagged with the FLAG epitope and expressed in HEK293 cells. Cell lysates from these cells were mixed and subjected to immunoprecipitation using beads coupled to anti-FLAG antibodies. Introducing the A4 mutation into full-length PTEN allowed to examine interactions of the core region of PTEN_{A4} and the C-terminal tail (Figures 2e–g). We found that PTEN_{C124S/A4} failed to bind to the C-terminal tail, but PTEN_{R130G/A4} maintained its binding ability (Figures 2f and g). Therefore, C124S impairs the ability of the core region to interact with the inhibitory tail, thereby stimulating membrane recruitment of PTEN.

The residue C124 can form a disulfide bond with another residue, C71, in the catalytic domain and disruption of this covalent bond has been proposed to target PTEN to the plasma membrane.⁹ However, we did not observe membrane recruitment of PTEN_{C71S} (Figures 2a and b). Therefore, the mechanism that recruits PTEN_{C124S} is not likely the break of the C124–C71 bond. To ameliorate the effects of various mutations on stability, we analyzed PTEN in the presence of MG132 for the remainder of this study.

As our screen isolated mutations near the C-terminal phosphorylation sites (Figure 1a, Y379, S380, T382, T383), we compared the role of each of the four phosphorylation sites (S380, T382, T383 and S385) in the membrane localization of PTEN. We found that substitutions of S380, T382 and T383 promoted membrane

localization of PTEN, whereas S385 did not (Figures 3a and b). In addition to the phosphorylation sites, the mutation Y379N greatly decreased phosphorylation of the C-terminal tail, suggesting that the inhibition of phosphorylation recruits PTEN_{Y379N} to the plasma membrane (Figure 3d). Furthermore, previous studies identified three additional residues (S362, T366 and S370), which were phosphorylated at the C-terminal region. However, we found that substitutions at these residues did not affect PTEN localization (Figures 3a and b). Finally, the phosphorylation mutations that increased membrane localization of PTEN also increased its nuclear localization (Figures 3a–c); therefore, the mechanisms that regulate PTEN membrane and nuclear localization may be related.

Our screen also isolated previously uncharacterized mutations that increase membrane localization (Figure 1a). First, the combination of two mutations, N262Y (located in the calcium-binding region 3 (CBR3) loop of the C2 domain) and N329H (located in the Cα2 loop of the C2 domain), increased membrane localization of PTEN, although each mutation alone was ineffective (Figures 4a and b). This increased membrane association was not due to decreased phosphorylation of the C-terminal domain (Figure 4c). Second, the mutation of K269E (located in the CBR3 loop), which alone did not affect membrane binding of PTEN, dramatically stimulated membrane localization in combination with the mutation of D381V (located near the C-terminal phosphorylation site), which alone only slightly increased membrane localization (Figures 4a and b). D381V decreased phosphorylation of the C-terminal tail, whereas K269E did not affect phosphorylation (Figure 4c). To test whether these amino acids are specifically coupled with each other, we examine the localization of PTEN_{N262Y,D381V} and PTEN_{K269E,N329H}, PTEN_{N262Y,K269E} and PTEN_{N329H,D381V}. All of the four mutants significantly enhanced membrane localization (Figures 4d and e). Among them, combinations of mutations in the tail domain with either the CBR3 loop (PTEN_{N262Y,D381V} and PTEN_{K269E,D381V}) or the Cα2 loop (PTEN_{N329H,D381V}) showed stronger effects. A combination of two mutations within the CBR3 loop showed relatively modest effects (PTEN_{N262Y,K269E}). It is likely that mutations in the C2 domain and the C-terminal tail additively stimulate membrane recruitment of PTEN.

The CBR3 loop contains five lysines, K260, K203, K266, K267 and K269, which interact with phosphatidylserine;^{12,20,21} however, their function in membrane recruitment has not been directly tested in cells. In addition, the loop is important for interactions with the C-terminal tail, as simultaneous substitution of all of the five lysine residues inhibits interactions of the core region with the tail domain.⁹ Our findings that PTEN_{N262Y,N329H} and PTEN_{K269E,D381V} increased membrane recruitment suggested that the mutations of N262Y and K269E may selectively block interactions with the tail domain but not with the membrane. Therefore, we thought that the roles of the CBR3 loop in core–tail interactions and in membrane association are separable. To test this idea, we substituted five lysines to alanines simultaneously and individually. When all of the lysines were replaced with alanine (PTEN_{CBR(K5A)}) or aspartate (PTEN_{CBR(K5D)}) neither molecule localized to the plasma membrane but both showed increased nuclear localization (Figures 4f and g). Furthermore, PTEN_{CBR(K5A)} and PTEN_{CBR(K5D)} remained to be defective in membrane localization, even if the A4 mutation was introduced into them (Figures 4h and i). However, not all of the lysines were required for membrane localization. Although individual mutations at K260, K263 and K267 almost completely abolished membrane localization of PTEN_{A4}, a mutation at K269 only partially decreased it (Figures 4h and i). In addition, nuclear localization was not affected by all of the individual lysine mutations in PTEN_{A4} (Figures 4h and i).

Next, we performed pull-down assays to examine the roles of the five lysines in interactions with the tail domain. PTEN_{A4}, but

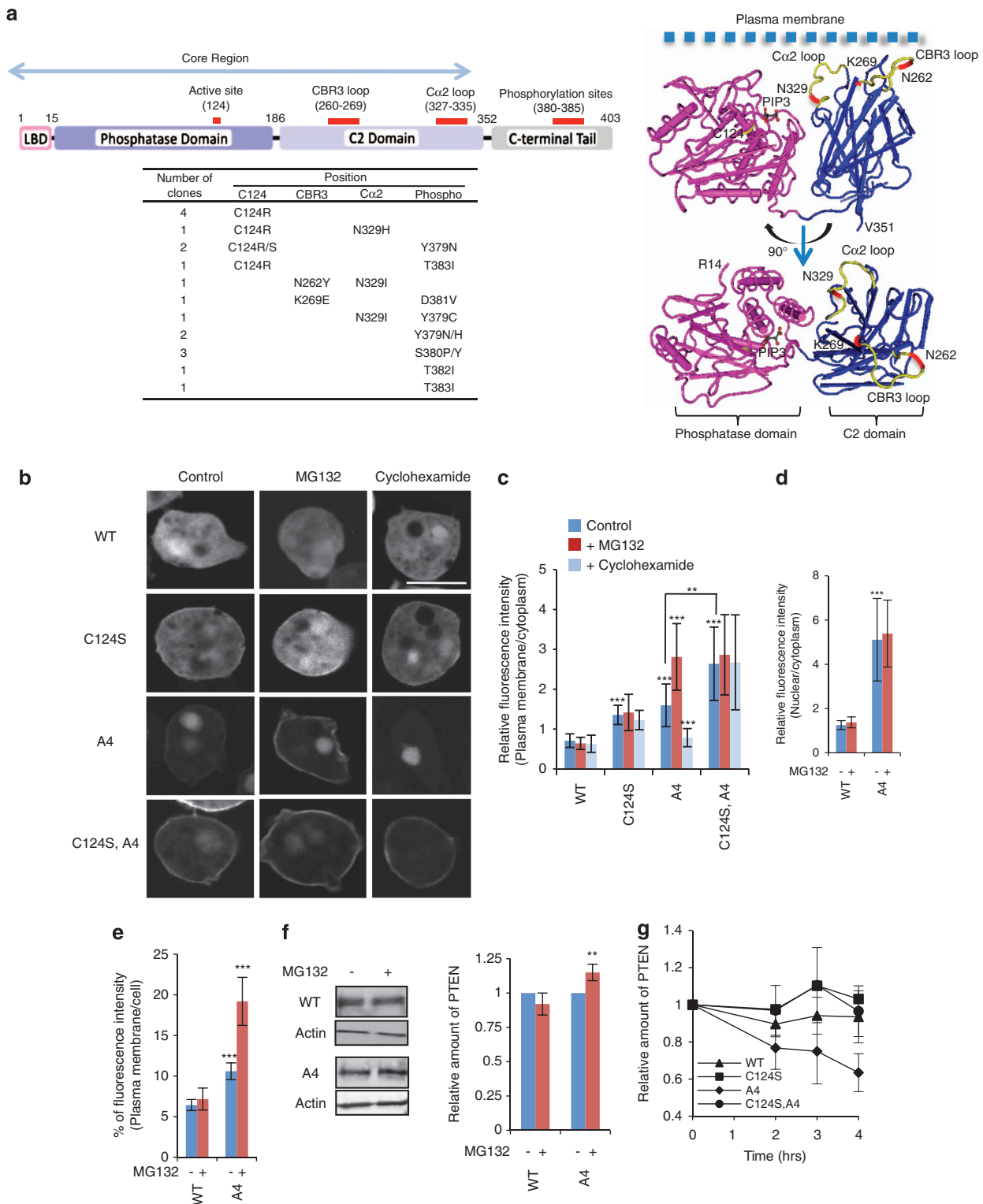


Figure 1. Isolated PTEN mutations. **(a)** The domain structure of PTEN is shown. The table summarizes the position and frequency of mutations isolated in the screen. The isolated mutations were indicated in the three dimensional structure of PTEN with the phosphatase and C2 domains (R14-V351)¹² (<http://www.ncbi.nlm.nih.gov/Structure/mmdbsrv.cgi?uid=11638>). **(b)** *Dictyostelium* cells expressing GFP fused to PTEN, PTEN_{C124S}, PTEN_{A4} and PTEN_{C124S,A4} were viewed by fluorescence microscopy. Cells were incubated in the presence or absence of 20 μM MG132 or 40 μg/ml cycloheximide. Bar, 10 μm. **(c, d)** Fluorescence intensity of GFP fused to WT or the indicated PTEN mutant at the plasma membrane **(c)** or nucleus **(d)** was quantified relative to that in the cytosol as described in Materials and Methods. Values represent the mean ± s.d. ($n \geq 15$). **(e)** Integrated fluorescence intensity of PTEN-GFP and PTEN_{A4}-GFP at the plasma membrane was normalized relative to total fluorescence intensity in cells ($n \geq 10$). **(f)** Whole-cell lysates prepared from cells expressing PTEN-GFP or PTEN_{A4}-GFP were analyzed by immunoblotting with antibodies against GFP and actin in the presence or absence of MG132. Band intensity was quantified ($n = 3$). **(g)** Cells expressing GFP fused to the indicated forms of PTEN were incubated with 40 μg/ml cycloheximide. Whole-cell lysates were analyzed by immunoblotting with anti-GFP antibodies at the indicated time points. Band intensity was quantified relative to 0 h sample ($n = 3$).

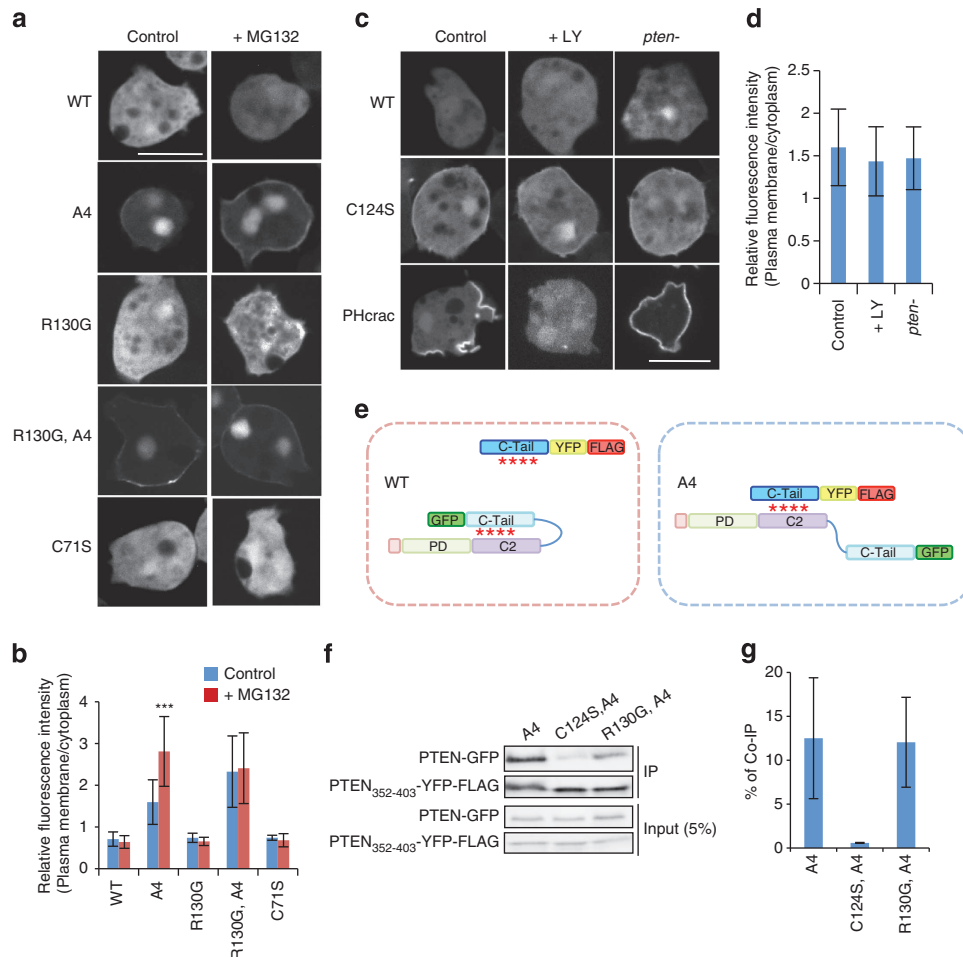


Figure 2. Analysis of PTEN_{C124S}. **(a)** *Dictyostelium* cells expressing GFP fused to PTEN, PTEN_{A4}, PTEN_{R130G}, PTEN_{R130G,A4} and PTEN_{C71S} were incubated with 20 μ M MG132 for 6 h and viewed using fluorescence microscopy. Bar, 10 μ m. **(b)** Fluorescence intensity at the plasma membrane was quantified ($n \geq 15$). **(c, d)** WT and PTEN-null cells expressing PTEN-GFP, PTEN_{C124S}-GFP or PHcrac-GFP were observed by fluorescence microscopy in the presence or absence of 20 μ M LY294002. Fluorescence intensity of PTEN_{C124S}-GFP at the plasma membrane was quantified **(d)**. Values represent the mean \pm s.d. ($n \geq 15$). **(e–g)** Interaction of the C-terminal tail domain of PTEN with full-length PTEN was assessed by pull-down assay. Whole-cell lysates expressing PTEN-GFP, PTEN_{C124S,A4}-GFP or PTEN_{R130G,A4}-GFP were incubated with PTEN₃₅₂₋₄₀₃-YFP-FLAG. Introducing the A4 mutation into full-length PTEN allowed to examine interactions of the core region of PTEN_{A4} and the C-terminal tail, as shown in **(e)**. PTEN₃₅₂₋₄₀₃-YFP-FLAG was immunoprecipitated with beads coupled to anti-FLAG antibodies. Bound fractions (immunoprecipitates, IP) were analyzed with antibodies to GFP and FLAG. **(g)** Band intensity was quantified ($n = 3$).

not WT PTEN, PTEN_{CBR(K5A),A4} or PTEN_{CBR(K5D),A4}, co-immunoprecipitated with the tail domain (Figure 4j). Individual substitution of the five lysines within the CBR3 loop showed that K260A, K263A, K267A and K269A, but not K266A, compromised interactions, with the strongest effect achieved by K269A (Figure 4k). Thus, K260, K263 and K267 may mediate interactions with both the membrane and the tail domain, whereas K269 mainly mediates interactions with the tail and only partially with the membrane. In addition to the lysine residues, N262 within the CBR3 loop may also selectively interact with the tail domain as the combination of the mutations N262Y and N329H blocked binding of the core region and to the tail domain (Figure 4j).

To study the function of PTEN, we examined the phosphatase activity of PTEN mutants. We immunopurified PTEN-GFP using beads coupled to anti-GFP antibodies and measured the phosphatase activity against a soluble form of PIP3, PIP3 diC8 (Figure 5a). C124S, R130G and C124S,A4 blocked the phosphatase activity, whereas CBR(K5A), CBR(K5D) and N262Y, N329H did not. Interestingly, A4 increased the phosphatase activity, suggesting that the C-terminal tail negatively regulates the activity, in addition to membrane localization. We further tested PTEN

function in cells by analyzing the ability to rescue PTEN-null *Dictyostelium* cells. Upon starvation, *Dictyostelium* cells move toward cAMP, aggregate and differentiate into multicellular structures called fruiting bodies that consist of spore and stalk cells (Figure 5b, WT).²² PTEN is necessary for chemotactic migration toward cAMP, and PTEN-null cells are defective in aggregation and differentiation (Figure 5b, vector).¹⁴ PTEN_{A4}, PTEN_{K269E,D381D} and PTEN_{N262Y,329H} reversed the developmental defects in the PTEN-null *Dictyostelium* cells, whereas PTEN_{C124S}, PTEN_{C124S,A4}, PTEN_{CBR3(K5A)} and PTEN_{CBR3(K5D)} did not (Figure 5b). However, the inability of PTEN_{CBR3(K5A)} and PTEN_{CBR3(K5D)} to rescue the PTEN-null phenotype was not due to the lack of the phosphatase activity (Figure 5a). Moreover, when we examined the effect of substitution of the five lysine residues in the CBR3 loop, K260A and K263A, which blocked membrane association, failed to rescue the developmental defects in PTEN-null cells, whereas K266A, K267A and K269A partially rescued the phenotype (Figure 5c), similar to their effects on the membrane association of PTEN_{A4} (Figures 5c and d). Therefore, our findings suggest that membrane recruitment is necessary for PTEN function.

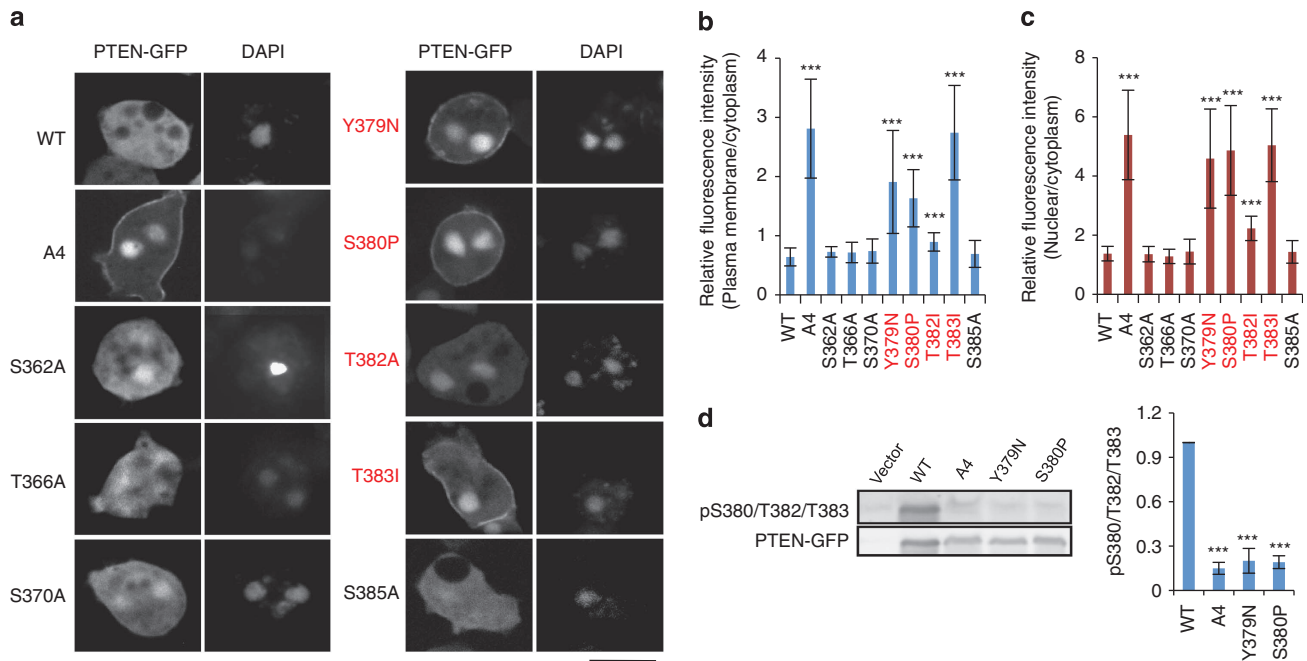


Figure 3. Mutational analysis of the C-terminal phosphorylation sites of PTEN. (a–c) *Dictyostelium* cells expressing GFP fused to the indicated version of PTEN were observed by fluorescence microscopy in the presence of 20 μ M MG132 (a). Bar, 10 μ m. GFP intensities at the plasma membrane (b) and nucleus (c) were determined relative to that in the cytosol. Values represent the mean \pm s.d. ($n \geq 15$). The mutations isolated from our screen are shown in red. (d) Whole-cell lysates expressing the indicated forms of PTEN-GFP were analyzed by immunoblotting with antibodies against phospho-PTEN (pS380/T382/T383) and GFP (PTEN-GFP). Band intensity was quantified ($n \geq 3$).

Finally, we validated our findings made in *Dictyostelium* cells by expressing WT and mutant forms of PTEN-GFP in HEK293T cells (Figure 6). Although WT PTEN is mainly located in the cytosol, PTEN_{C124C} and PTEN_{A4} increased association with the plasma membrane, consistent with previous reports. Combination of C124 and A4 further recruited PTEN_{C124S,A4} to the membrane. Moreover, the new substitutions that we isolated in this study (K269E, D381V and N262Y, N329H) promoted membrane localization of PTEN in HEK293T cells, as observed in *Dictyostelium* cells.

DISCUSSION

In this study, we showed that heterologous expression in *Dictyostelium* cells enabled a rapid visual inspection of PTEN localization in single colonies with efficient recovery of plasmids to identify mutations by DNA sequencing. Expression of human PTEN in *Dictyostelium* cells allows improved visualization of membrane localization relative to mammalian cells, a simple readout of overall function, and the ability to carry out random mutagenesis. With this system, we have defined mechanisms that control membrane localization of human PTEN. Furthermore, taking advantage of the fact that human PTEN functionally replaces *Dictyostelium* PTEN, we demonstrated the functional importance of membrane recruitment of human PTEN in cells.

On the basis of our findings, we propose that the CBR3 loop, the C2 loop and the catalytic domain form a membrane-binding regulatory interface at one surface of the PTEN protein (Figure 7). Supporting our model, the membrane-binding regulatory interface can be seen in the crystal structure of the PTEN molecule (Figure 1a). The three lysines at residues 260, 263 and 267 in the CBR3 loop are critical for the membrane association and function of PTEN in cells. These positively charged residues may directly form a bridge with negatively charged phospholipid head groups in the plasma

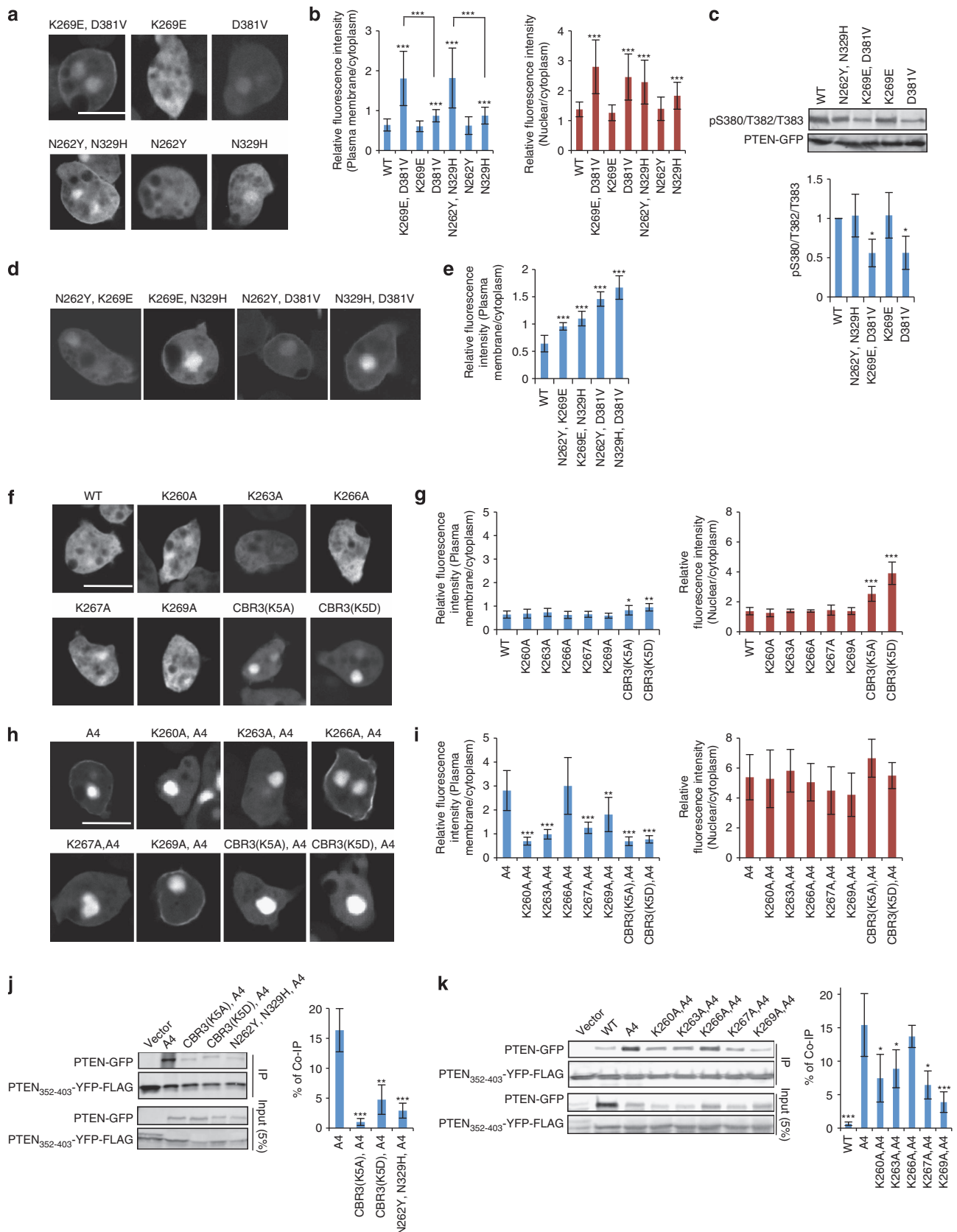
membrane (Figure 7). Consistent with this model, a previous biochemical study showed that the CBR3 loop is necessary for the interactions of PTEN with phosphatidylserine.^{12,20,21}

The CBR3 loop is also important for interaction with the inhibitory C-terminal tail domain (Figure 7). Thus, the positively charged CBR3 loop may bind to phosphates at residues S380 and T383 in the tail domain. Previous studies have suggested that in this 'closed' form of the enzyme, the membrane-binding capacity is blocked by steric hindrance. We show that the C α 2 loop, which contains the residue N329, and the catalytic domain do not appear to directly interact with the membrane. Instead, these regions strengthen interactions with the C-terminal tail. Similarly, the lysine at 269 in the CBR3 loop appears to mainly mediate interactions with the tail domain but not with the membrane. The C-terminal tail domain dissociates from the CBR3 loop upon dephosphorylation, allowing the face of the protein including the C3 loop to bind to the membrane. The C-terminal tail can not only block membrane association, it can also inhibit enzymatic activity, as PTEN_{A4} had higher phosphatase activity. Our model envisions that opening the conformation of PTEN provides its robust activation by releasing the inhibitory effects of the tail domain on both its localization and activity.

It has been shown that interactions of the C-terminal tail with the core region are important for the stability of PTEN.¹⁸ Our current study supports this model and further shows that PTEN_{A4} is degraded by proteasomes and this degradation requires its phosphatase activity. We speculate that phosphorylation of PTEN may inhibit this mechanism, whereas auto-dephosphorylation by PTEN may release this inhibition and stimulate degradation of PTEN by proteasomes. It is currently unknown which phosphorylated residues mediate this regulation. It is also possible that PTEN degradation is coupled to its enzymatic action at the plasma membrane. This coupling could potentially serve as a clock that determines the timeframe in which PTEN is

active at the membrane, which would help sustain intracellular PIP3 signaling. It would be interesting to speculate that this degradation mechanism is modified by phosphatidylinositol in the

plasma membrane, providing feedback from the level of PIP3 and/or phosphatidylinositol (4,5)-bisphosphate. Interactions with these phosphatidylinositols may control the conformation of PTEN and



target PTEN for degradation. Finally, nuclear localization of PTEN may help protect PTEN from degradation by sequestering the protein from the degradation machinery at the membrane.

MATERIALS AND METHODS

Cell culture and plasmids

All *Dictyostelium* cells were cultured in HL5 medium at 22 °C. Cells expressing PTEN-GFP were selected by G418 (20 µg/ml), LY294002 (20 µM), MG132 (20 µM) and cycloheximide (40 µg/ml) were used to inhibit PI3K, proteasomes and protein synthesis, respectively. The PCR primers and plasmids used in this study are listed in Supplementary Tables S1 and S2, respectively. Human PTEN was mutagenized using overlap extension PCR as previously described²³ and cloned into pKF3, a *Dictyostelium* expressing plasmid carrying GFP. All constructs were confirmed by DNA sequencing. HEK293T cells were maintained in Dulbecco's Modified Eagle medium (Invitrogen, Carlsbad, CA, USA) supplemented with 10% fetal bovine serum (Invitrogen). Cells were transiently transfected with 1 µg of DNA plasmids on eight-well chambered coverglass (Lab-TekII, Nunc, Rochester, NY, USA) using 3 µl of GeneJuice

(Novagen, Darmstadt, Germany), following the manufacturer's protocol. Cells were then incubated for 24 h before observation.

Isolation of PTEN mutants that show enhanced membrane localization

Human PTEN complementary DNA was randomly mutagenized using a Diversity PCR random mutagenesis kit (Clontech, Mountain View, CA, USA). The PCR products were cloned into the pKF3 plasmid and electroporated into MegaX DH10B competent cells (Invitrogen). More than 120 000 bacterial colonies were collected. Ten of the mutagenized plasmids were sequenced to check distribution and diversity of mutations. The extracted plasmids were pooled to create the PTEN library and electroporated into *Dictyostelium* cells.^{14,24} More than 20 000 transformants were collected and cultured under shaking condition in the presence of G418 for 5 days. Cells were plated on five 96-well optical plates (Thermo Scientific, Waltham, MA, USA) at a density of 1000 cells/well. After 3 days, cells with increased membrane localization of PTEN-GFP were manually picked up by a pipette under a Zeiss HAL100 epifluorescence inverted microscope equipped with a × 40 objective and transferred to new wells. This isolation process was repeated until cells with increased membrane localization of PTEN comprise

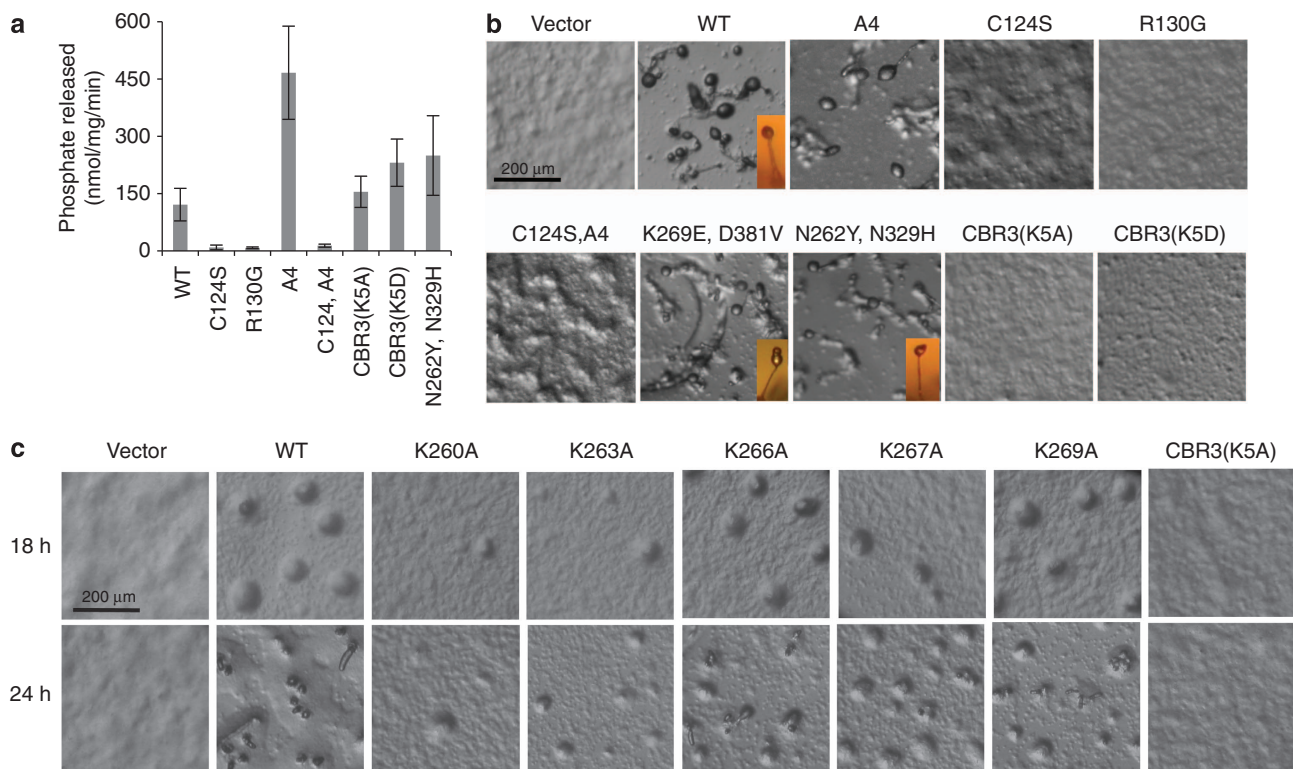


Figure 5. PTEN requires membrane association and phosphatase activity for its function. **(a)** The indicated PTEN-GFP proteins were immunopurified from *Dictyostelium* cells, and phosphatase activities were measured ($n \geq 3$). **(b, c)** PTEN-null *Dictyostelium* cells expressing different PTEN-GFP constructs were starved to induce differentiation into fruiting bodies. Pictures were taken at 36 h **(b)** and 18 and 22 h **(c)** after the onset of starvation. Although PTEN-null cells expressing PTEN (WT) formed fruiting bodies, PTEN-null cells expressing a vector alone did not aggregate and remained undifferentiated **(b)**. Inserts show side views of fruiting bodies **(b)**.

Figure 4. The CBR3 and Cα2 loops are important for interactions with the plasma membrane and the C-terminal tail. **(a, b)** *Dictyostelium* cells expressing the indicated forms of PTEN-GFP were viewed by fluorescence microscopy in the presence of 20 µM MG132 **(a)**. Intensities of GFP signals at the plasma membrane and nucleus were quantified relative to that in the cytosol **(b)**. Bar, 10 µm. **(c)** Whole-cell lysates expressing GFP fused to different forms of PTEN were analyzed by immunoblotting with antibodies against phospho-PTEN (pS380/T382/T383) and GFP (PTEN-GFP). Band intensity was quantified ($n \geq 3$). **(d, e)** Cells expressing the indicated versions of PTEN-GFP were examined in the presence of 20 µM MG132 **(d)**. Fluorescence intensity of GFP at the plasma membrane was quantified **(e)**. Values represent the mean ± s.d. ($n \geq 15$). **(f, g)** GFP fused to PTEN with the indicated mutations in the CBR3 loop were expressed in *Dictyostelium* cells in the presence of 20 µM MG132 **(f)**. Relative GFP signals at the plasma membrane and nucleus were determined relative to that in the cytosol **(g)**. **(h, i)** GFP fused to PTEN_{A4} with the indicated CBR3 loop mutations were expressed in *Dictyostelium* cells in the presence of 20 µM MG132 **(h)**. Relative GFP signals at the plasma membrane and nucleus were determined relative to that in the cytosol **(i)**. **(j, k)** Interaction of the C-terminal domain of PTEN carrying mutations in the CBR3 and Cα2 loops with its N-terminal core region was assessed in pull-down assays. PTEN_{352–403}-YFP-FLAG was added to whole-cell lysates expressing the indicated PTEN-GFP constructs and immunoprecipitated with beads coupled to anti-FLAG antibodies. Bound fractions (IP) were analyzed with antibodies to GFP and FLAG. Band intensity was quantified ($n = 3$).

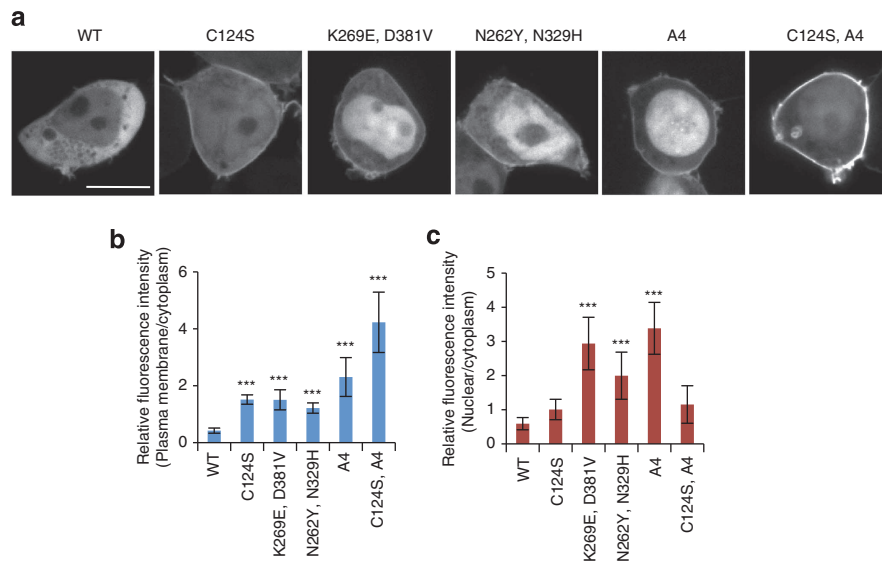


Figure 6. Localization of GFP-PTEN in HEK293T cells. HEK293T cells expressing the indicated forms of PTEN-GFP were viewed by fluorescence microscopy (**a**). (**b**, **c**) Intensities of GFP signals at the plasma membrane (**b**) and nucleus (**c**) were quantified relative to that in the cytosol (**b**). Bar, 10 μ m.

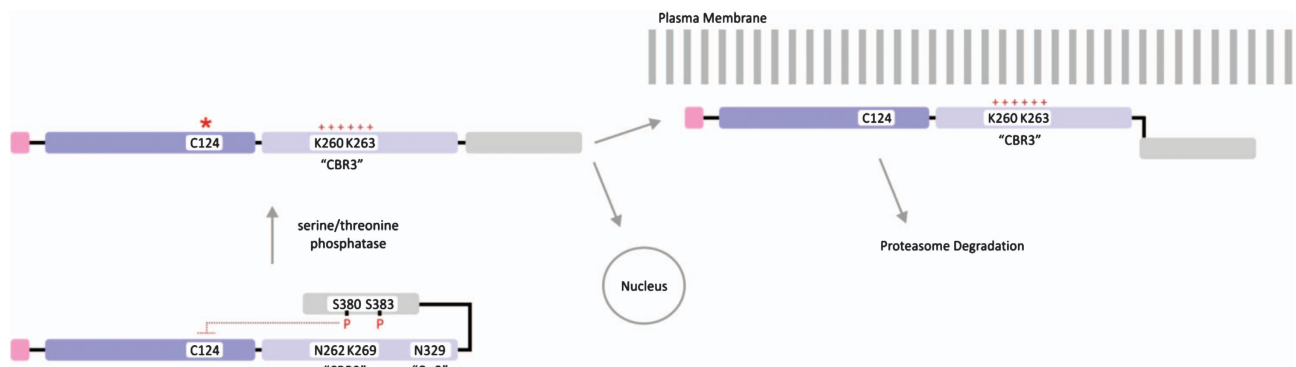


Figure 7. Model for mechanisms of PTEN membrane localization. Positively charged lysine residues (K260, K263 and K269) in the CBR3 loop are masked by phosphorylated serine (S380) and threonine (T383) in the C-terminal tail. PTEN adopts an open conformation upon dephosphorylation of the tail, and the two lysine residues interact with negatively charged phospholipids in the plasma membrane. Proteasome-mediated degradation of PTEN occurs rapidly at the plasma membrane and is dependent upon the phosphatase activity of PTEN. The open conformation of dephosphorylated PTEN would also expose an otherwise hidden nuclear localization signal to promote nuclear import of PTEN.

about 50–70% of the total cell population in each well. To isolate individual clones, cells were plated on SM agar with *Klebsiella aerogenes*. After 5 days, individual plaques from SM plates were transferred to the optical plate and confirmed for enhancement of membrane association of PTEN-GFP. To identify mutations that resulted in increased membrane localization, the PTEN gene isolated from individual clones was PCR-amplified and sequenced. To identify mutations that are responsible for enhanced membrane localization, mutations were separated by subcloning a DNA fragment of the PTEN gene. In some cases, single mutations were created in the PTEN gene using site-directed mutagenesis with overlap extension PCR.

Confocal microscopy and quantification of PTEN-GFP localization
To observe PTEN-GFP, cells were washed with DB and placed on eight-well chambered coverglass (Lab-TekII, Nunc). Fluorescent images were acquired under a Leica DMI 6000 inverted microscope equipped with a $\times 63$ objective and captured by a CoolSNAP EZ camera. All images were analyzed using Image J software (NIH, Bethesda, MD, USA). To quantify fluorescence intensity of PTEN-GFP at the plasma membrane and nucleus relative to the cytosol, we measured and averaged fluorescence intensity in 1 pixel area from three different positions in each compartment. Background fluorescence intensity was subtracted from each measurement. The nucleus was identified by 4',6-

diamidino-2-phenylindole staining. To integrate fluorescence intensity of PTEN-GFP at the plasma membrane, the total intensity at the cell periphery was measured and normalized relative to that in the cytosol.

Developmental assay

PTEN-null *Dictyostelium* cells were grown exponentially (4×10^5 cells/ml), washed twice in DB (10 mM phosphate buffer, 2 mM MgSO_4 , 0.2 mM CaCl_2) and plated on 1% non-nutrient DB agar for 36 h.^{25,26} Cells were observed under an Olympus SZ-PT dissecting microscope equipped with $\times 6$ objective and their images were taken by a Nikon 4500 camera.

Assays for interactions between PTEN and its C-terminal tail

Interactions between PTEN and its C-terminal tail (PTEN_{352–403}-YFP-FLAG) were examined, as described.⁹ HEK293T cells were cultured in Dulbecco's Modified Eagle medium supplemented with 10% fetal bovine serum on a 100-mm dish, transiently transfected with 8 μ g of the plasmid carrying PTEN_{352–403}-YFP-FLAG using GeneJuice (Novagen) and then cultured for 24 h in Dulbecco's Modified Eagle medium with 10% fetal bovine serum. HEK293T cells were lysed in 1 ml of lysis buffer containing 1% Nonidet P-40, 50 mM NaCl, 20 mM Tris-HCl (pH 7.5), 10% glycerol, 0.1 mM EDTA,

phosphatase inhibitor cocktail (Sigma, St Louis, MO, USA) and protease inhibitor cocktail (Roche, Upper Bavaria, Germany). The lysates were then cleared by centrifugation at 13 000 r.p.m. for 20 min at 4 °C. *Dictyostelium* cells expressing WT and mutant versions of PTEN-GFP were lysed in 1% Nonidet P-40, 300 mM NaCl, 10 mM Tris-HCl (pH 7.5), 2 mM EDTA, phosphatase inhibitor cocktail (Sigma) and protease inhibitor cocktail (Roche). The lysates were then cleared by centrifugation at 13 000 r.p.m. for 20 min at 4 °C. Hundred microlitres of the HEK293T lysates were mixed with 500 µl of the *Dictyostelium* lysates. Beads coupled to anti-FLAG antibodies (Sigma) were added to the mixtures and incubated for 2 h. The beads were washed twice in the lysis buffer and the bound fractions were analyzed by SDS–polyacrylamide gel electrophoresis and immunoblotting using antibodies to FLAG and GFP.

Immunoblotting

Proteins were resolved by SDS–polyacrylamide gel electrophoresis and transferred onto polyvinylidene difluoride membrane. Antibodies against PTEN (138G6, Cell Signaling, Danvers, MA, USA), phosphorylated PTEN at residues S380, T382 and T383 (44A7, Cell Signaling), GFP (11E5, Molecular Probes, Carlsbad, CA, USA) and actin (C-11, Santa Cruz Biotechnology, Santa Cruz, CA, USA) were used. Immunocomplexes were visualized by fluorophore-conjugated secondary antibodies including anti-rabbit Alexa Fluoro 488 (Invitrogen), anti-goat Alexa Fluoro 647 (Invitrogen) and anti-mouse Dylight 649 (Jackson ImmunoResearch Lab, West Grove, PA, USA) and detected using a PharosFX Plus molecular imager (Bio-Rad, Hercules, CA, USA).

In vitro phosphatase activity assay

The phosphatase activity of PTEN was measured, as described previously.¹⁷ WT and mutant forms of PTEN fused to GFP were expressed in *Dictyostelium* cells and immunopurified using GFP-Trap agarose beads (Allele Biotech, San Diego, CA, USA). The phosphatase activity was determined by measuring the release of phosphates from PIP3 diC8 using a Malachite Green Phosphatase assay kit (Echelon, Salt Lake City, UT, USA). The activity was normalized to amounts of purified PTEN-GFP proteins.

Statistical analysis

P-values were determined using the Student's *t*-test: **P* < 0.05; ***P* < 0.01; ****P* < 0.001.

CONFLICT OF INTEREST

The authors declare no conflict of interest.

ACKNOWLEDGEMENTS

This work was supported by NIH grants to MI (GM084015), PND (GM28007 and GM34933) and HS (GM089853 and NS084154). We thank M Rahdar and KF Swaney for providing plasmids.

REFERENCES

- Hollander MC, Blumenthal GM, Dennis PA. PTEN loss in the continuum of common cancers, rare syndromes and mouse models. *Nat Rev Cancer* 2011; **11**: 289–301.
- Carracedo A, Alimonti A, Pandolfi PP. PTEN level in tumor suppression: how much is too little? *Cancer Res* 2011; **71**: 629–633.

- Leslie NR, Dixon MJ, Schenning M, Gray A, Batty IH. Distinct inactivation of PI3K signalling by PTEN and 5-phosphatases. *Adv Biol Regul* 2012; **52**: 205–213.
- Rodon J, Dienstmann R, Serra V, Tabernero J. Development of PI3K inhibitors: lessons learned from early clinical trials. *Nat Rev Clin Oncol* 2013; **10**: 143–153.
- Vanhaesebroeck B, Stephens L, Hawkins P. PI3K signalling: the path to discovery and understanding. *Nat Rev Mol Cell Biol* 2012; **13**: 195–203.
- Baker SJ. PTEN enters the nuclear age. *Cell* 2007; **128**: 25–28.
- Song MS, Salmena L, Pandolfi PP. The functions and regulation of the PTEN tumour suppressor. *Nat Rev Mol Cell Biol* 2012; **13**: 283–296.
- Tamguney T, Stokoe D. New insights into PTEN. *J Cell Sci* 2007; **120**(Pt 23): 4071–4079.
- Rahdar M, Inoue T, Meyer T, Zhang J, Vazquez F, Devreotes PN. A phosphorylation-dependent intramolecular interaction regulates the membrane association and activity of the tumor suppressor PTEN. *Proc Natl Acad Sci USA* 2009; **106**: 480–485.
- Walker SM, Leslie NR, Perera NM, Batty IH, Downes CP. The tumour-suppressor function of PTEN requires an N-terminal lipid-binding motif. *Biochem J* 2004; **379**(Pt 2): 301–307.
- Dennning G, Jean-Joseph B, Prince C, Durden DL, Vogt PK. A short N-terminal sequence of PTEN controls cytoplasmic localization and is required for suppression of cell growth. *Oncogene* 2007; **26**: 3930–3940.
- Lee JO, Yang H, Georgescu MM, Di Cristofano A, Maehama T, Shi Y *et al*. Crystal structure of the PTEN tumor suppressor: implications for its phosphoinositide phosphatase activity and membrane association. *Cell* 1999; **99**: 323–334.
- Das S, Dixon JE, Cho W. Membrane-binding and activation mechanism of PTEN. *Proc Natl Acad Sci USA* 2003; **100**: 7491–7496.
- Iijima M, Devreotes P. Tumor suppressor PTEN mediates sensing of chemoattractant gradients. *Cell* 2002; **109**: 599–610.
- Vazquez F, Matsuoka S, Sellers WR, Yanagida T, Ueda M, Devreotes PN. Tumor suppressor PTEN acts through dynamic interaction with the plasma membrane. *Proc Natl Acad Sci USA* 2006; **103**: 3633–3638.
- Iijima M, Huang YE, Devreotes P. Temporal and spatial regulation of chemotaxis. *Dev Cell* 2002; **3**: 469–478.
- Iijima M, Huang YE, Luo HR, Vazquez F, Devreotes PN. Novel mechanism of PTEN regulation by its phosphatidylinositol 4,5-bisphosphate binding motif is critical for chemotaxis. *J Biol Chem* 2004; **279**: 16606–16613.
- Vazquez F, Ramaswamy S, Nakamura N, Sellers WR. Phosphorylation of the PTEN tail regulates protein stability and function. *Mol Cell Biol* 2000; **20**: 5010–5018.
- Myers MP, Pass I, Batty IH, Van der Kaay J, Stolarov JP, Hemmings BA *et al*. The lipid phosphatase activity of PTEN is critical for its tumor suppressor function. *Proc Natl Acad Sci USA* 1998; **95**: 13513–13518.
- Shenoy S, Shekhar P, Heinrich F, Daou MC, Gericke A, Ross AH *et al*. Membrane association of the PTEN tumor suppressor: molecular details of the protein-membrane complex from SPR binding studies and neutron reflection. *PLoS One* 2012; **7**: e32591.
- Lumb CN, Sansom MS. Defining the membrane-associated state of the PTEN tumor suppressor protein. *Biophysical J* 2013; **104**: 613–621.
- Fey P, Kowal AS, Gaudet P, Pilcher KE, Chisholm RL. Protocols for growth and development of *Dictyostelium discoideum*. *Nat Protoc* 2007; **2**: 1307–1316.
- Zhang P, Wang Y, Sesaki H, Iijima M. Proteomic identification of phosphatidylinositol (3,4,5) triphosphate-binding proteins in *Dictyostelium discoideum*. *Proc Natl Acad Sci USA* 2010; **107**: 11829–11834.
- Chen CL, Wang Y, Sesaki H, Iijima M. Myosin I Links PIP3 signaling to remodeling of the actin cytoskeleton in chemotaxis. *Sci Signaling* 2012; **5**: ra10.
- Cai H, Huang CH, Devreotes PN, Iijima M. Analysis of chemotaxis in *Dictyostelium*. *Methods Mol Biol* 2012; **757**: 451–468.
- Wang Y, Steimle PA, Ren Y, Ross CA, Robinson DN, Egelhoff TT *et al*. *Dictyostelium huntingtin* controls chemotaxis and cytokinesis through the regulation of myosin II phosphorylation. *Mol Biol Cell* 2011; **22**: 2270–2281.

Supplementary Information accompanies this paper on the Oncogene website (<http://www.nature.com/onc>)